

1 Identification of magnetic anomalies based on ground 2 magnetic data analysis using multifractal modeling: A case 3 study in Qoja-Kandi, East Azerbaijan Province, Iran

4
5 E. Mansouri¹, F. Feizi², and A. A. Karbalaeei Ramezanali¹

6 [1]{Young Researchers and Elite Club, South Tehran Branch, Islamic Azad
7 University, Tehran, Iran}

8 [2]{Mine Engineering Department, South Tehran Branch, Islamic Azad University, Tehran,
9 Iran}

10 Correspondence to: F.Feizi (feizi.faranak@yahoo.com)

11 12 **Abstract**

13 Ground magnetic anomaly separation using Reduction-To-the-Pole (RTP) technique and the
14 fractal concentration-area (C-A) method has been applied to the Qoja-Kandi prospecting area
15 in NW Iran. The geophysical survey resulting in the ground magnetic data was conducted for
16 magnetic elements exploration. Firstly, RTP technique was applied for recognizing
17 underground magnetic anomalies. RTP anomalies was classified in to different populations
18 based on the current method. For this reason, drilling point areas determination by RTP
19 technique was complicated for magnetic anomalies, which is in the center and north of
20 studied area. Next, C-A method was applied on the RTP-Magnetic-Anomalies (RTP-MA) for
21 demonstrating magnetic susceptibility concentrations. This identification was appropriate for
22 increasing the resolution of the drilling point areas determination and decreasing the drilling
23 risk issue, due to the economic costs of underground prospecting. In this study, the results of
24 C-A Modeling on the RTP-MA are compared with 8 borehole data. The results shows that
25 there is a good correlation between anomalies derived via C-A method and log report of
26 boreholes. Two boreholes were drilled in magnetic susceptibility concentrations, based on
27 multifractal modeling data analyses, between 63533.1 to 66296 nT. Drilling results showed
28 appropriate magnetite thickness with grades greater than 20% Fe. Total associated with
29 anomalies containing andesite units host iron mineralization.

1 **1 Introduction**

2 Mineral exploration aims at **discovering** new mineral deposits in a region of interest (Abedi et
3 al., 2013). These mineral deposits could be related to magnetic anomalies which are **situated**
4 **within** underground. In the first **step** of identification underground magnetic anomalies, few
5 boreholes should be drilled after interpretation Ground magnetic data. Obviously, using new
6 methods could increase the resolution of the **drilling point areas** determination and decrease
7 the drilling risk. A cursory look at magnetic maps **would present more information** about the
8 shape of **such a** buried features. However, **the information acquired from** map can provide
9 additional details about the specification of underground magnetic anomalies especially exact
10 **locations. Magnetic anomaly depends on the inclination and declination of the body's**
11 **magnetization generally. Also we know that the orientation of the magnetic body depends to**
12 **magnetic north. According to the mentioned issues (Baranov, 1957) and (Baranov and Naudy,**
13 **1964) proposed a mathematical approach known as reduction-to-the-pole (RTP) for**
14 **simplifying anomaly shape and determining anomaly exact location.** As a result of increasing
15 the resolution of RTP technique, concentration-area (C-A) fractal method was applied. Fractal
16 geometry is a Non-Euclidean geometry established by Mandelbrot (1983) and has been
17 applied in geosciences and mineral exploration, especially in geophysical and geochemical
18 exploration since 1980s, (Turcotte (1989), Bolviken et al. (1992), Korvin (1992), Cheng et al.
19 (1994), Agterberg et al. (1996), Cheng (1999), Turcotte (2004), Dimri (2005) and Shen et al.
20 (2009)).

21 In this study, concentration-area (C-A) fractal method was used to gridded RTP data set, for
22 better classification of RTP map which generated from RTP technique. This procedure was
23 applied to the ground magnetic data of Qoja-Kandi, Zanjan Province, Iran.

24

25 **2 The concentration-area fractal method**

26 The concentration-area (C-A) method serves to illustrate the **correlated** relationship between
27 the obtained results. Its most useful features are the easy implementation and the ability to
28 compute quantitative anomalous thresholds (Cheng et al., 1994).

29 Cheng et al. (1994) proposed the concentration–area (C–A) method for separating
30 geochemical anomalies from background in order to characterize the distribution of elemental
31 concentrations. Equations (1) Shows the general form of this model.

1 $A(\rho \leq \gamma) \propto \rho^{-a_1}; A(\rho \geq \gamma) \propto \rho^{-a_2} \quad (1)$

2 Where $A(\rho)$ denotes the area with concentration values greater than the contour value
3 ρ ; γ represents the threshold; and a_1 and a_2 are characteristic exponents. The breaks between
4 straight line segments in C-A log-log plot and the corresponding values of ρ are known as
5 thresholds to separate geophysical values into different components representing different
6 causal factors such as, lithological differences, geochemical processes and mineralizing
7 events (Lima et al., 2003). Thus, applying C-A fractal model to the geochemical data,
8 improves resolution of the data helping to explore the deposits. It seems that, applying this
9 model to ground magnetic data improves the accuracy of magnetite deposit exploration. The
10 most useful feature of the C-A method is its capability to compute anomaly thresholds
11 (Goncalves et al., 2001). Using fractal theory, Cheng et al. (1994) derived similar power-law
12 relationships and equations in extended form. The area $A(\rho)$ for a given ρ is equal to the
13 number of cells multiplied by cell area with concentration values greater than ρ . Average
14 concentration values are used for those boxes containing more than one sample. Area-
15 concentration [$A(\rho)$] with element concentrations greater than ρ usually shows a power-law
16 relation (cheng et al., 1994).

17 **3 The study area and geological setting**

18 The Qoja-Kandi area is located within the Orumieh-Dokhtar magmatic arc in northwest
19 of Iran (Fig. 1); This magmatic arc is the most important **exploratory area** for metals, and
20 hosts the majority of the larger metals deposits such as copper and iron (Hassan-Nezhad and
21 Moore, 2006) The investigated area characterized by Precambrian to Jurassic units and Oligo-
22 Miocene volcanic rocks. Different types of metal ore deposits, such as iron have already
23 been documented near studied area. The lithology of this part includes schist and shale
24 (Kahar formation), dolomite and limestone (Elika formation), shale, sandstone and limestone
25 (Shemshak formation), limestone, marl, sandstone, conglomerate and andesite. A magnetite
26 dyke which has outcrops in andesite units has already been seen near studied area. It seems
27 that this magnetite dyke presence in Qoja-Kandi area.

28

1 **4 Ground magnetic data analysis**

2 Ground magnetic data are acquired in the region at 15 m spacing along lines in the north
3 direction and spaced 10 m apart. 6997 geophysical ground data were collected by GSM-
4 19T proton. **GSM-19T proton magnetometer has absolute accuracy +/- 0.2 nT.**

5 **4.1 The TMI anomaly map**

6 The Total-Magnetic-Intensity (TMI) map of the Qoja-Kandi area was obtained to delineate
7 the subsurface anomaly. Fig. 2 indicates TMI with ground magnetic data points. The ground
8 magnetic anomalies range from 38633 to 69509 nT and are characterized by both low and
9 high frequencies of anomalies. The map reveals that dipolar (anomalies having positive and
10 negative components) magnetic anomalies have a general E-W direction, which is in the
11 center and north of studied area. There are three obvious dipolar magnetic anomalies (two
12 anomalies in the east and west of the center and one anomaly in the north) in the Qoja-Kandi
13 prospecting area which are expected to depend on two magnetite dyke in andesite units.

14 **4.2 Reduction to the pole technique**

15 **A difficulty in interpretation with** TMI anomalies is that they are dipolar (anomalies having
16 positive and negative components) such that the shape and phase of the anomaly depends **on**
17 **the part of** magnetic inclination and the presence of any remanent magnetization. Because of
18 depending magnetic anomaly on the inclination and declination of the body's magnetization,
19 the inclination and declination of the local earth's magnetic field, and the orientation of the
20 body with respect to magnetic north,(Baranov, 1957) and (Baranov and Nudy, 1964)
21 proposed a mathematical approach known as reduction to the pole for simplifying anomaly
22 shape.

23 The reduction-to-the-pole (RTP) technique transforms TMI anomalies to anomalies that
24 would be measured if the field were vertical (assuming there is only an inducing field). This
25 RTP transformation makes the shape of magnetic anomalies more closely related to the
26 spatial location of the source structure and makes the magnetic anomaly easier to interpret, as
27 anomaly maxima will be located centrally over the body (provided there is no remanent
28 magnetization present). Thus, the RTP reduces the effect of the Earth's ambient magnetic field
29 and provides a more accurate determination of the position of anomalous sources. It is

1 therefore understood that the total magnetization direction is equivalent to that of the current
2 inducing field.

3 Before applying the methods, the total field anomaly data were converted to RTP using a
4 magnetic inclination of 55.43° and a declination of 4.93° . RTP anomalies, shows three
5 obvious magnetic anomalies (two anomalies in the east and west of the south and one
6 anomaly in the north) in the studied area, elongated in approximate E-W direction. The
7 highest class of RTP-Magnetic-Anomalies (RTP-MA) based on Reduction to the pole
8 technique is > 55370.7 nT with 24941.79 square meters area. Also, RTP anomalies was
9 classified to different populations based on this method, as illustrated in Fig. 3. Based on this
10 method, drilling points determination with RTP technique was complicated.

11 **4.3 Application of C-A Modeling on the RTP-MA**

12 Multifractal models are utilized to quantify patterns such as geophysical data. Fractal and
13 multifractal modeling are widely applied to distinguish the different mineralized zones
14 (Cheng, 2007). Multifractal theory could be interpreted as a theoretical framework that
15 explains the power law relationships between areas enclosing concentrations below a given
16 threshold value and the actual concentrations itself. To demonstrate and prove that data
17 distribution has a multifractal nature, an extensive computation is required (Halsey et al.,
18 1986). This method has several constrains especially when the boundary effects on irregular
19 geometrical data sets are involved (Agterberg et al., 1996; Goncalves, 2001; Cheng, 2007;
20 Xie et al., 2010). Multifractal modelings in geophysical and geochemical exploration help to
21 find exploration targets and mineralization potentials in different types of deposits (Yao and
22 Cheng, 2011). The C-A method seems to be equally applicable to all cases which means that
23 geophysical distributions mostly satisfy the properties of a multifractal function. There is
24 some evidence that geophysical and geochemical data distributions have fractal behavior in
25 nature, e.g. Bolviken et al. (1992), Turcotte (1997), Goncalves (2001), Gettings (2005) and Li
26 and Cheng (2006). This theory improves the development of an alternative interpretation
27 validation and useful methods to be applied to geophysical distributions analysis.

28 In this study, 57307 transformed RTP data were processed for identification of magnetic
29 anomalies. Statistical results reveal that RTP-MA mean value is 48441 nT, as depicted in Fig.
30 4, and the RTP-MA domain shows a wide range. **C-A Modeling overcomes the distortion effects
31 of outliers on the traditional techniques and makes it unnecessary to determine whether the**

1 concentration data are drawn from a normal (i.e., Gaussian) distribution or log-normal distribution,
2 and this advances the analysis resolution of anomalies (Fig. 5). RTP-MA distribution map was
3 generated with minimum curvature method. The estimated RTP-MA model in terms of RTP
4 data values was intended to build of the C-A log-log plot for RTP-MA. Based on linear
5 segments and breakpoints log-log plot, as shown in Fig. 6, geophysical population were
6 divided. RTP threshold values are 45383, 47424.2, 49493.7, 56493.7 and 635331.1 which are
7 very low, low, moderate, high and very high intensity anomaly threshold values, respectively,
8 as illustrated in Table 1. Pairs of estimated exponents and corresponding optimum thresholds
9 for RTP-MA are presented in Table 2. The thresholds delineate anomalous areas. Comparison
10 of the areas above and below the threshold of 6022 nT on the contour map (Fig. 3) with the
11 RTP map shows significant spatial correlation between the areas with RTP-MA concentration
12 above 6022 nT. These geophysical populations were determined based on the breakpoints in
13 log-log plot. Actually the length of the tangent, demonstrate the extents of geophysical
14 populations in fractal model. It is mentioned that the number of population in fractal model
15 could be more or less than five, but actually the extent of the last class population isn't highly
16 dependent on the number of population in fractal model. Hence, there are five populations for
17 RTP-MA which illustrate that fifth class of RTP-MA based on fractal method is > 63533.1 nT
18 with very high priority for drilling. Consequently, the locations of RTP-MA (two anomalies)
19 based on fractal method are situated in the east of southern part of the area, as depicted in Fig.
20 7.

21 **5 Control with borehole data**

22 A method of investigating subsurface geology is, of course, drilling boreholes. For a more
23 accurate results about identification of magnetic anomalies, the results of C-A Modeling on
24 the RTP-MA are compared with borehole data (Table 3). There are 8 drilled boreholes in this
25 area that are used for identification of magnetic anomalies obtained from boreholes (Fig. 8).
26 The drilled boreholes were analyzed and studied by geologists. Hence, range of magnetite
27 ores in each borehole were obtained and documented as log report in Table 2. The accepted
28 lower limit for the ore length, is the grade 20% Fe total.

29 RTP transformed data based on ground magnetic anomaly data collected from C-A moderate
30 anomalies in Qoja-Kandi prospecting area show magnetic susceptibility concentration
31 between 63533.1 to 66296 nT with 1957.64 m² area. This study shows that the areas with
32 very high priority obtained by C-A method have magnetite concentration with appropriate

1 thickness. This point is significant that borehole 1 and 2 were drilled in mentioned places and
2 confirmed the results of C-A model (Fig. 9) for increasing the resolution of drilling point
3 determination and decreasing the drilling risk. Fig. 8 shows 3D RTP map of Qoja-Kandi
4 based on C-A method with pictures from magnetite zones in the surface of drilled borehole1
5 and 2, in addition of mentioned boreholes log plots. It is necessary to mention that, the
6 TERRA satellite has a back-looking telescope with a resolution of 15 m in the VNIR that
7 matches with the wavelength of the band 3 that is used to extract 3D information for provided
8 Fig. 9.

9 The results confirmed there is affirmative correlation between anomalies derived via C-A
10 method and log report of boreholes. Furthermore, the ratio of the ore length and total core
11 length is calculated in Table 3. The number of this ratio is between ranges of 0 to 1. Whatever
12 this number is larger and close to 1, the resolution of the drilling point determination increase
13 and the drilling risk decrease. The results shows positive correlation between the ratio of the
14 ore and total core column, and Priority areas for drilling column. Based on this study,
15 anomalies associated with andesite units host iron mineralization. Also, there isn't any
16 mineralization in other geological units such as limestones and conglomerates in northwest of
17 the studied area. It should be noted that, magnetite ores have outcrops in andesite units (Fig.
18 9).

19 **6 Conclusions**

20 Separation of magnetic anomalies using combine of RTP technique and C-A fractal modelling
21 has been used in Qoja-Kandi prospecting area as a new geophysical method for increasing the
22 resolution of the drilling points determination. This study demonstrates that C-A method
23 utilizing for ground magnetic anomaly separation is an appropriate manner for geophysical
24 prospecting.

25 There was a multifractal model for RTP-MA, based on Log-log plots in the prospecting
26 area. In this paper, RTP anomalies results from C-A method and RTP technique were
27 compared. Anomalies resulting from RTP technique show huge anomalies in three parts, but
28 C-A method show two small anomalies. RTP anomalies based on RTP technique are similar
29 to anomalies from C-A method because of normal distribution in Qoja-kandi area. According
30 to correlation between geological particulars and RTP anomalies obtained from C-A method,
31 andesite units host the anomalies in the studied area.

1 There is an appropriate correlation between the calculated anomalous threshold values and ore
2 thicknesses in total cores. Also, the ratio of the ore length and total core length is related to
3 anomalous threshold, calculated with C-A method. Based on RTP technique, three anomalies
4 (two RTP anomalies were identified in the east and west of the southern part of the area and
5 one anomaly in the northern part). Also, according to the C-A method, two small anomalies
6 are situated in the east of southern part of the prospecting area with very high priority for
7 drilling. Borehole 1 and 2 were drilled in mentioned places and confirmed the results of C-A
8 model for increasing the resolution of drilling point determination and decreasing the drilling
9 risk.

10 Hence study geophysical magnetic anomalies with the C-A method can be a proper way for
11 geophysicists to find targets with enriched magnetic elements. Also, applying C-A log-log can
12 increase the resolution of the drilling point determination and decrease the drilling risk.

13

1 **References**

- 2 Abedi, M., Torabi, S.A., Norouzi, G.H.: Application of fuzzy AHP method to integrate
3 geophysical data in a prospect scale, a case study: Seridune copper deposit, *Boll. Geofisica*
4 *Teorica Appl*, 54, 145–164, 2013.
- 5 Agterberg, F. P., Cheng, Q., Brown, A., and Good, D.: Multifractal modeling of fractures in
6 the Lac du Bonnet batholith, Manitoba, *Comput. Geosci.*, 22, 497–507, 1996.
- 7 Arian, M.: Physiographic-Tectonic Zoning of Iran's Sedimentary Basins, *Open Journal of*
8 *Geology*, 3, 169-177, 2013.
- 9 Baranov, V., Naudy, H.: Numerical calculation of the formula of reduction to the magnetic
10 pole, *Geophysics*, 29, 67-79, 1964.
- 11 Baranov, V.: A new method for interpretation of aeromagnetic maps; pseudo-gravimetric
12 anomalies, *Geophysics*, 22, 359-382, 1957.
- 13 Bolviken, B., Stokke, P. R., Feder, J., and Jossang, T.: The fractal nature of geochemical
14 landscapes, *J. Geochem. Explor.*, 43, 91–109, 1992.
- 15 Cheng, Q., Agterberg, F. P., and Ballantyne, S. B.: The separation of geochemical anomalies
16 from background by fractal methods, *J. Geochem. Explor.*, 51, 109–130, 1994.
- 17 Cheng, Q.: Multifractal imaging filtering and decomposition methods in space, Fourier
18 frequency, and eigen domains, *Nonlin. Processes Geophys.*, 14, 293–303, doi:10.5194/npg
19 14-293-2007, 2007.
- 20 Cheng, Q.: Spatial and scaling modelling for geochemical anomaly separation, *J. Geochem.*
21 *Explor.*, 65, 175–194, 1999.
- 22 Dimri, V. P.: *Fractal Behavior of the Earth System*, The Netherlands, Springer, 208 pp., 2005.
- 23 Gettings, M. E.: Multifractal magnetic susceptibility distribution models of hydrothermally
24 altered rocks in the Needle Creek Igneous Center of the Absaroka Mountains, Wyoming,
25 *Nonlin. Processes Geophys.*, 12, 587–601, doi:10.5194/npg-12-587- 2005, 2005.
- 26 Goncalves, M. A., Mateus, A., and Oliveira, V.: Geochemical anomaly separation by
27 multifractal modeling, *J. Geochem. Explor.*, 72, 91–114, 2001.

- 1 Halsey, T. C., Jensen, M. H., Kadanoff, L. P., Procaccia, I., and Shraiman, B. I.: Fractal
2 measures and their singularities: The characterization of strange sets. *Phys. Rev. A*, 33, 1141
3 1151, 1986.
- 4 Hassan-Nezhad, A. A., Moore, F.: A stable isotope and fluid inclusion study of the Qaleh-Zari
5 Cu–Au–Ag deposit, Khorasan Province, Iran, *Journal of Asian Earth Sciences.*, 27, 805–818,
6 2006.
- 7 Korvin, G.: *Fractal Models in the Earth Science*, Elsevier, Amsterdam, 396 pp., 1992.
- 8 Li, Q. and Cheng, Q.: VisualAnomaly: A GIS-based multifractal method for geochemical and
9 geophysical anomaly separation in Walsh domain, *Comput. Geosci.*, 32, 663–672, 2006.
- 10 Lima, A., De Vivo, B., Cicchella, D., Cortini, M., and Albanese, S.: Multifractal
11 IDWinterpolation and fractal filtering method in environmental studies: an application on
12 regional stream sediments of (Italy), Campania region, *Appl. Geochem.*, 18, 1853–1865,
13 2003.
- 14 Mandelbrot, B. B.: *The Fractal Geometry of Nature*, W. H. Freeman, San Fransisco, 468 pp.,
15 1983.
- 16 Shen, W., Fang, C., and Zhang, D.: Fractal and Chaos Research of Geomagnetic Polarity
17 Reversal, *Earth Sci. Front.*, 16, 201–206, 2009.
- 18 Turcotte, D. L.: *Fractals and Chaos in Geology and Geophysics*, Cambridge University Press,
19 Cambridge, 398 pp., 1997.
- 20 Turcotte, D. L.: Fractals in geology and geophysics, *Pure Appl. Geophys.*, 131, 171–196,
21 1989.
- 22 Turcotte, D. L.: The relationship of fractals in geophysics to “the new science”, *Chaos*,
23 *Soliton. Fract.*, 19, 255–258, 2004.
- 24 Xie, S., Cheng, Q., Zhang, S., and Huang, K.: Assessing microstructures of pyrrhotites in
25 basalts by multifractal analysis, *Nonlin. Processes Geophys.*, 17, 319–327, doi:10.5194/npg
26 17- 319-2010, 2010.
- 27 Yao, L. and Cheng, Q.: Multi-scale interactions of geological processes during
28 mineralization: cascade dynamics model and multifractal simulation, *Nonlin. Processes*
29 *Geophys.*, 18, 161–170, doi:10.5194/npg-18-161-2011, 2011.
- 30

1 Table 1. RTP classification of magnetic anomalies based on fractal method.

2

Class ID	Classes range (nT)	Priority areas for drilling
1	45383 – 47424.2	Very low
2	47424.2 – 49493.7	Low
3	49493.7 – 56493.7	Moderate
4	56493.7 – 63533.1	High
5	63533.1 - 66296	Very high

3

1 Table 2. Results obtained by using the power law method and weights of evidence procedure;
2 α_1 and α_2 are the exponents of the power-law relation for concentration values less and greater
3 than the threshold value (v), respectively.

4

Total magnetic intensity	v	Power law		W. of T
		α_1	α_2	v
RTP(nT)	60022	0.0116	0.0458	60022

5

6

7

8

9

10

11

12

13

14

15

16

17

18

19

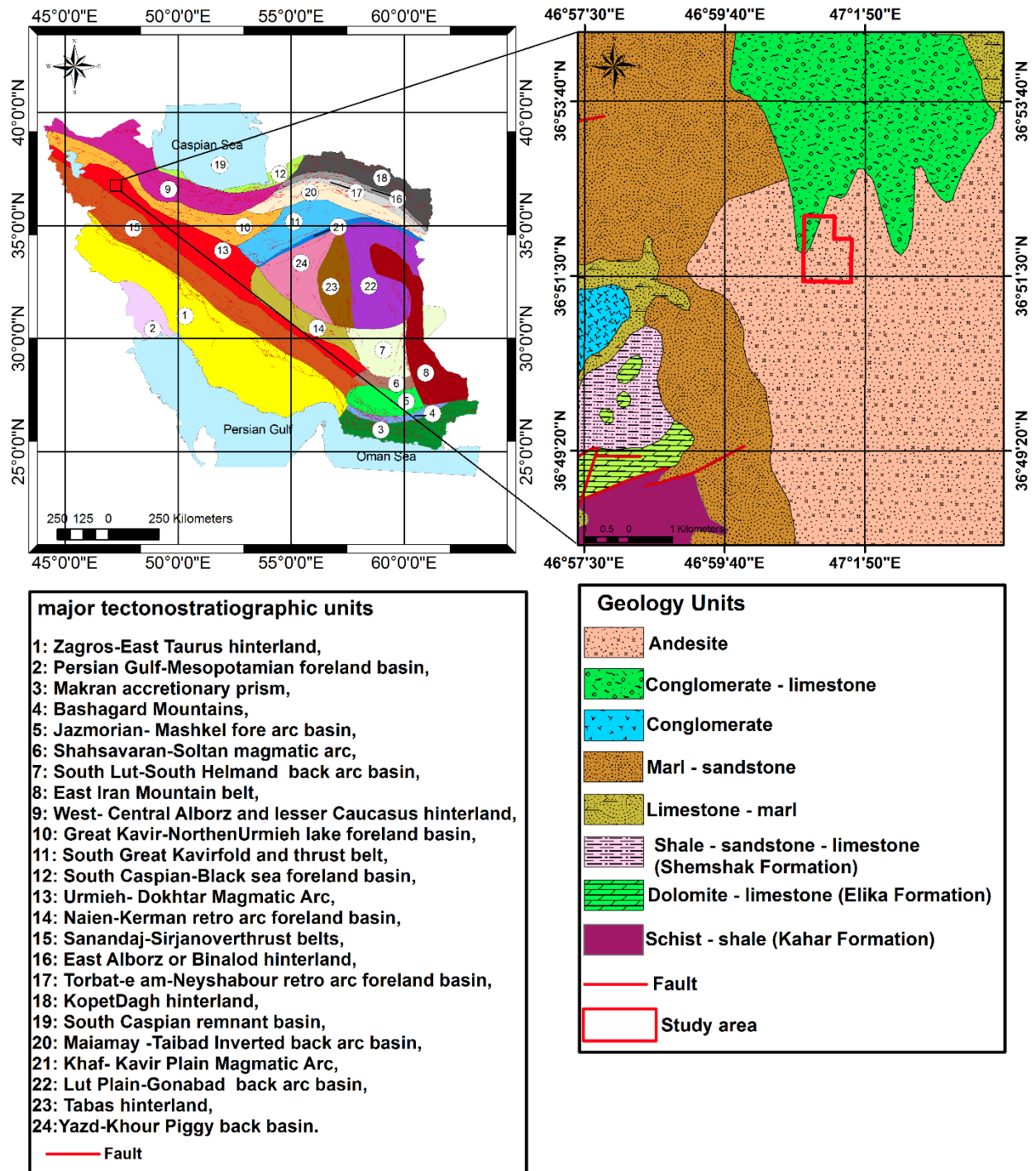
20

21

1 Table 3. Log report of boreholes with RTP classification based on fractal method.

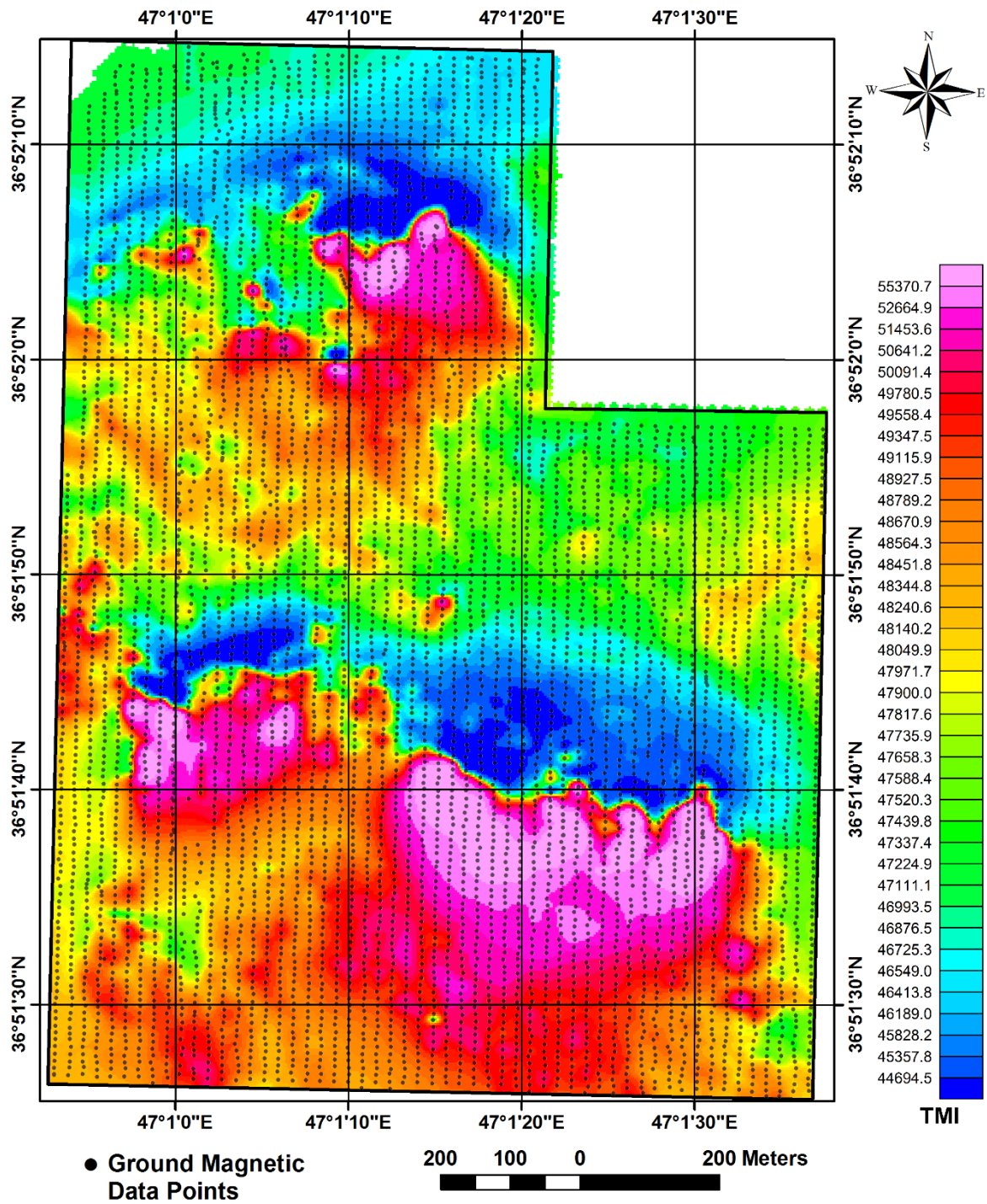
2

Borehole ID	Total core (m)	Magnetite thickness (m) in total core(grades greater than 20% Fe total)		Magnetite range (m)		Priority areas for drilling
		Ore core	Total core	From	To	
BH1	136.5	52.4	0.38	19.3	25.2	Very high
				60.7	85.2	
BH2	171.2	47.2	0.27	109.4	131.4	Very high
				4	12.2	
BH3	151.2	32	0.21	50.2	53.5	High
				130.6	166.3	
BH4	106	12.5	0.11	80	102	Moderate
				112	122	
BH5	58.9	0	0	44	48	Very low
				81	89.5	
BH6	136.5	3	0.02	-	-	Low
				69	72	
BH7	172	14	0.08	44	47	Moderate
				61.5	63.5	
BH8	157	29	0.18	156	164	High
				70	90	
				133	142	



1
2
3
4
5

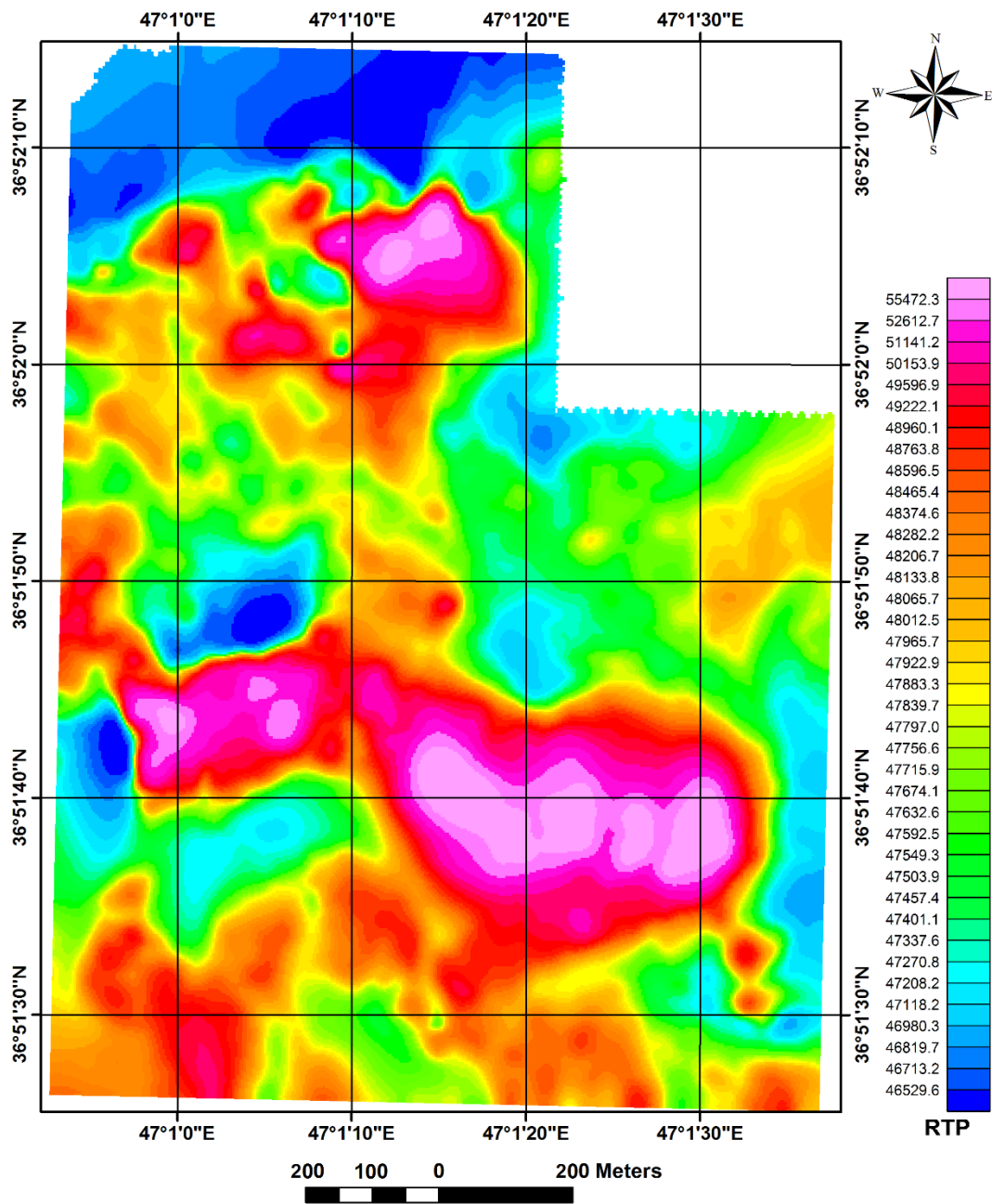
Figure 1. Physiographic-tectonic zoning map of Iran's sedimentary basins (Arian, 2013) and location of study area.



1

2

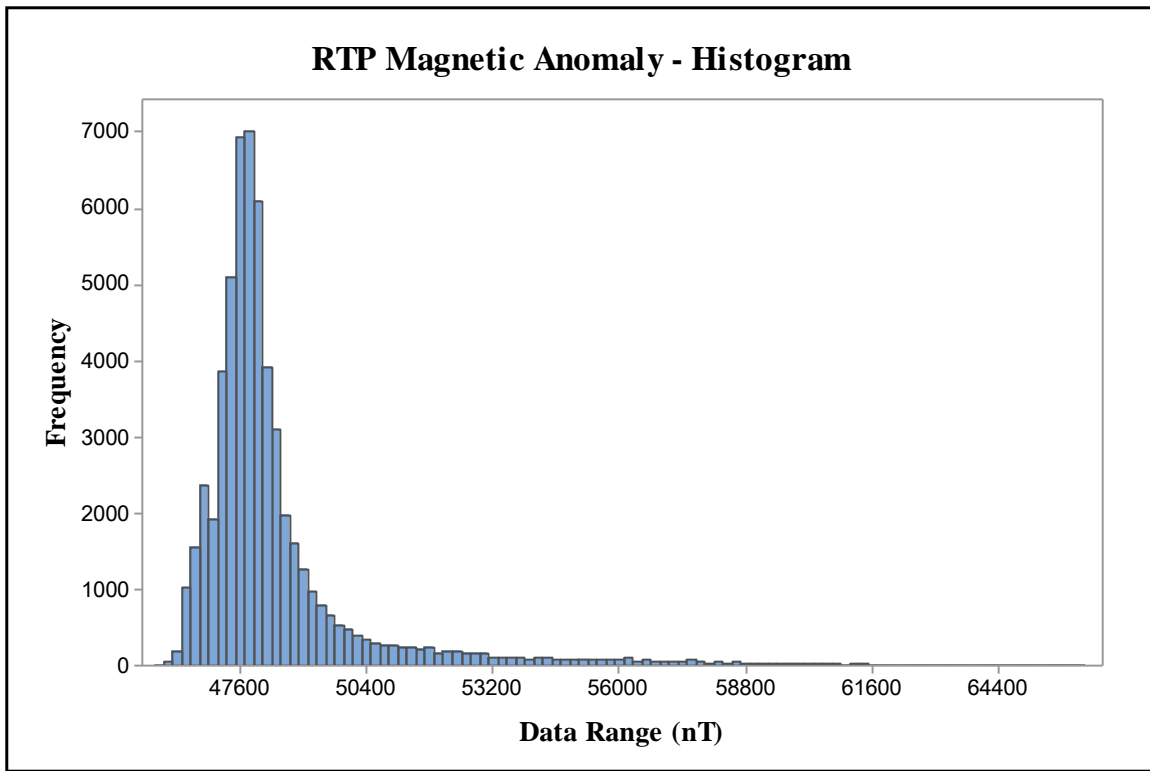
3 Figure 2. TMI map of Qoja-Kandi with ground magnetic data points.



1

2

3 Figure 3. RTP map of Qoja-Kandi based on Reduction to the pole technique.



1

2

3 **Figure 4. Histogram of RTP-MA data in Qoja-Kandi.**

4

5

6

7

8

9

10

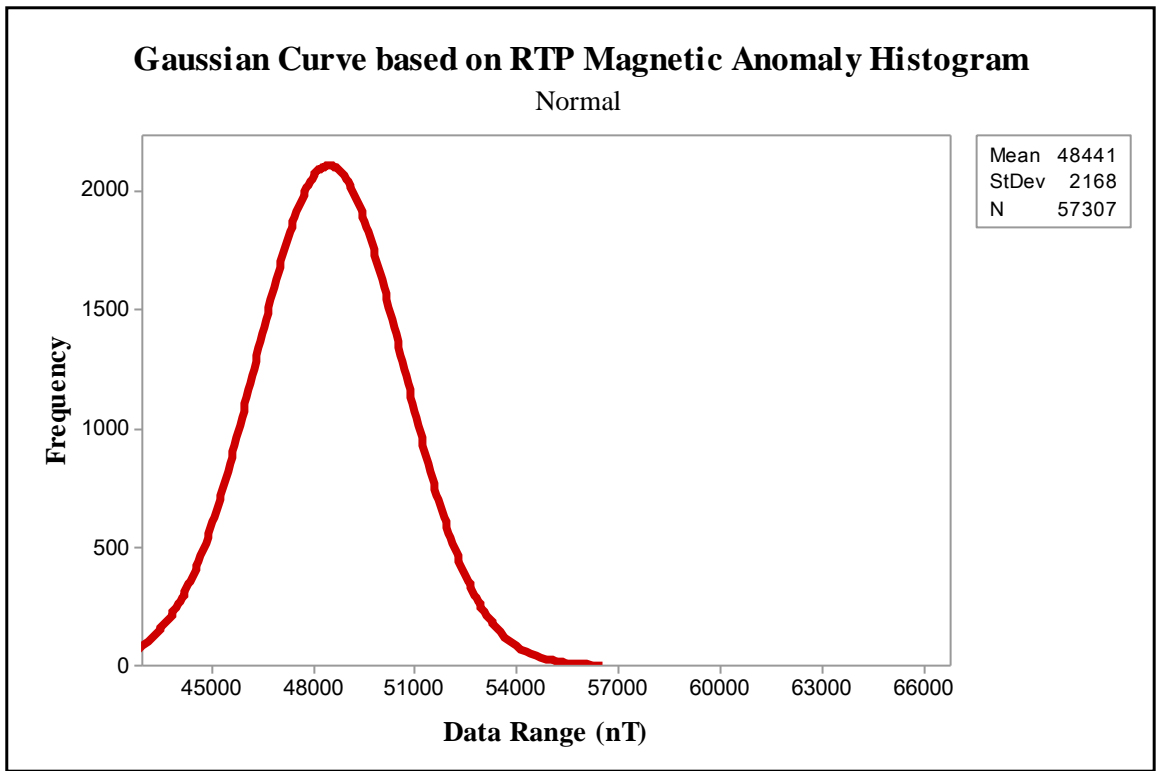
11

12

13

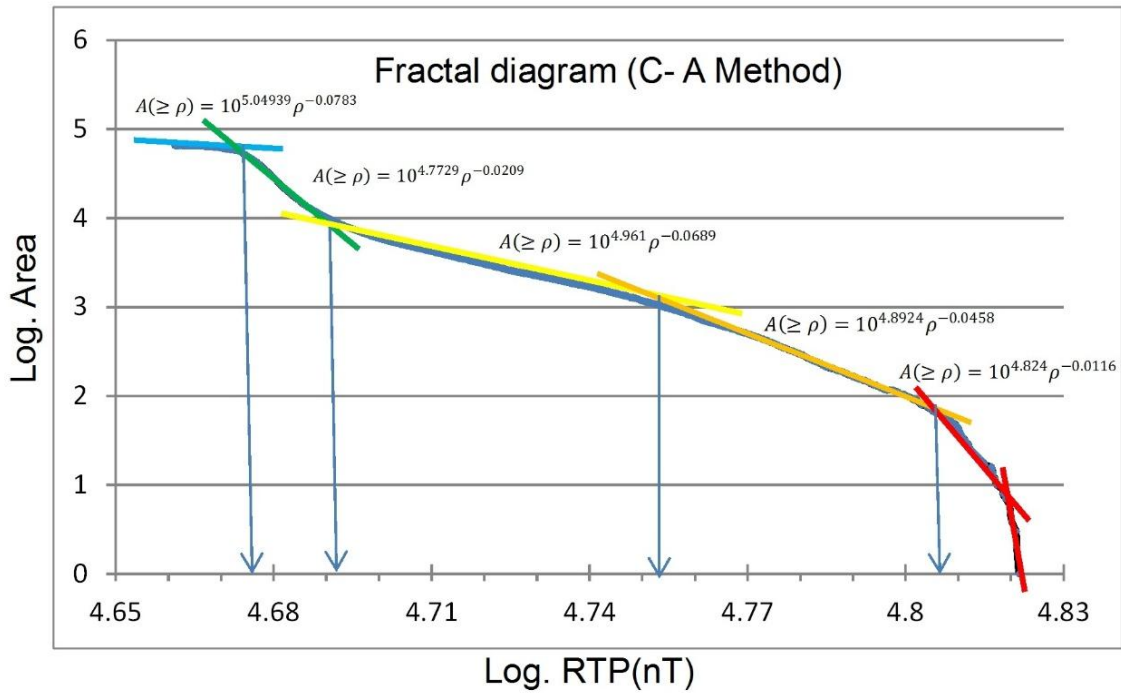
14

15



1
2
3
4
5
6
7
8

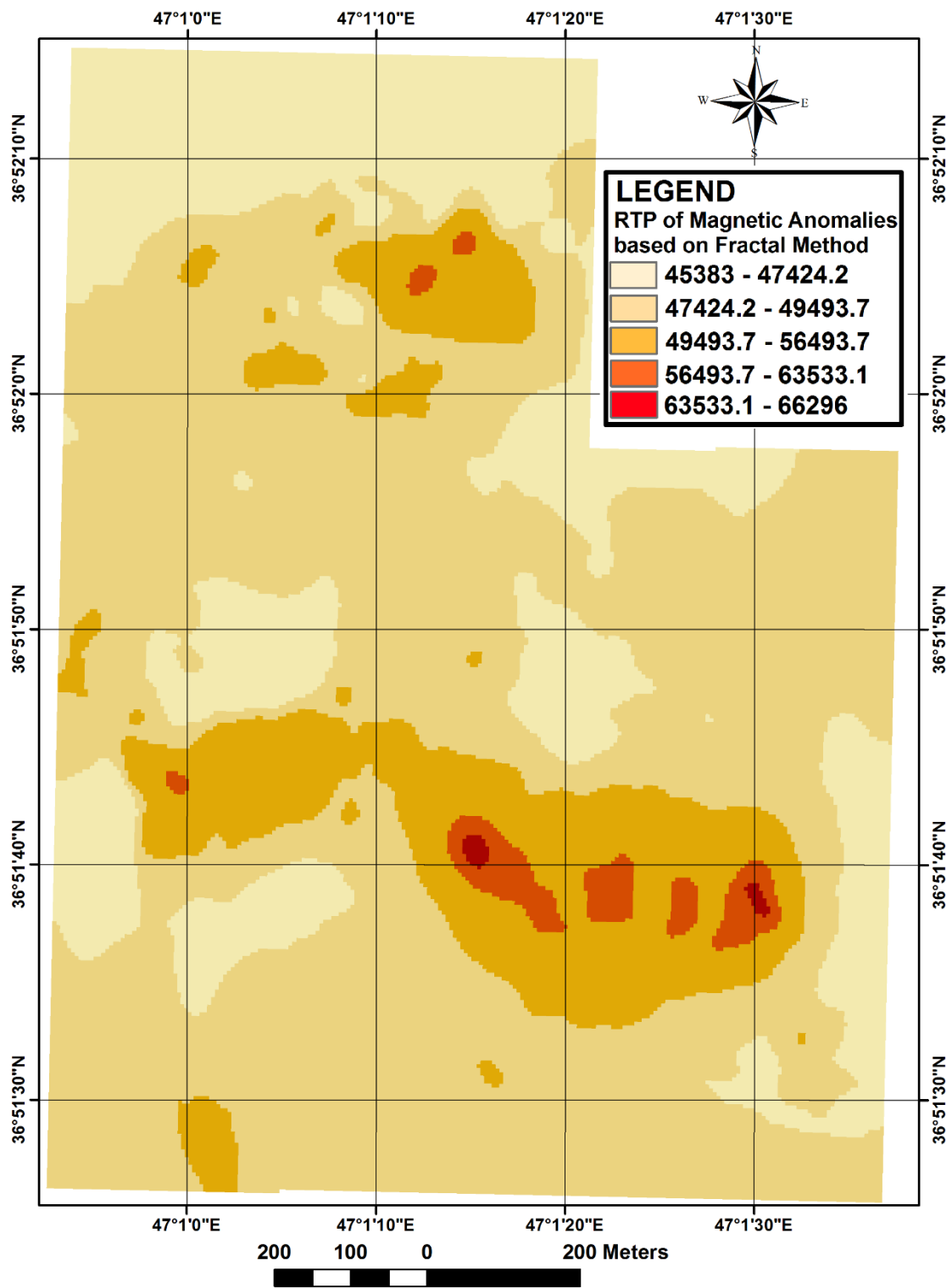
Figure 5. Gaussian curve based on RTP Magnetic anomaly histogram in Qoja-Kandi.



1

2

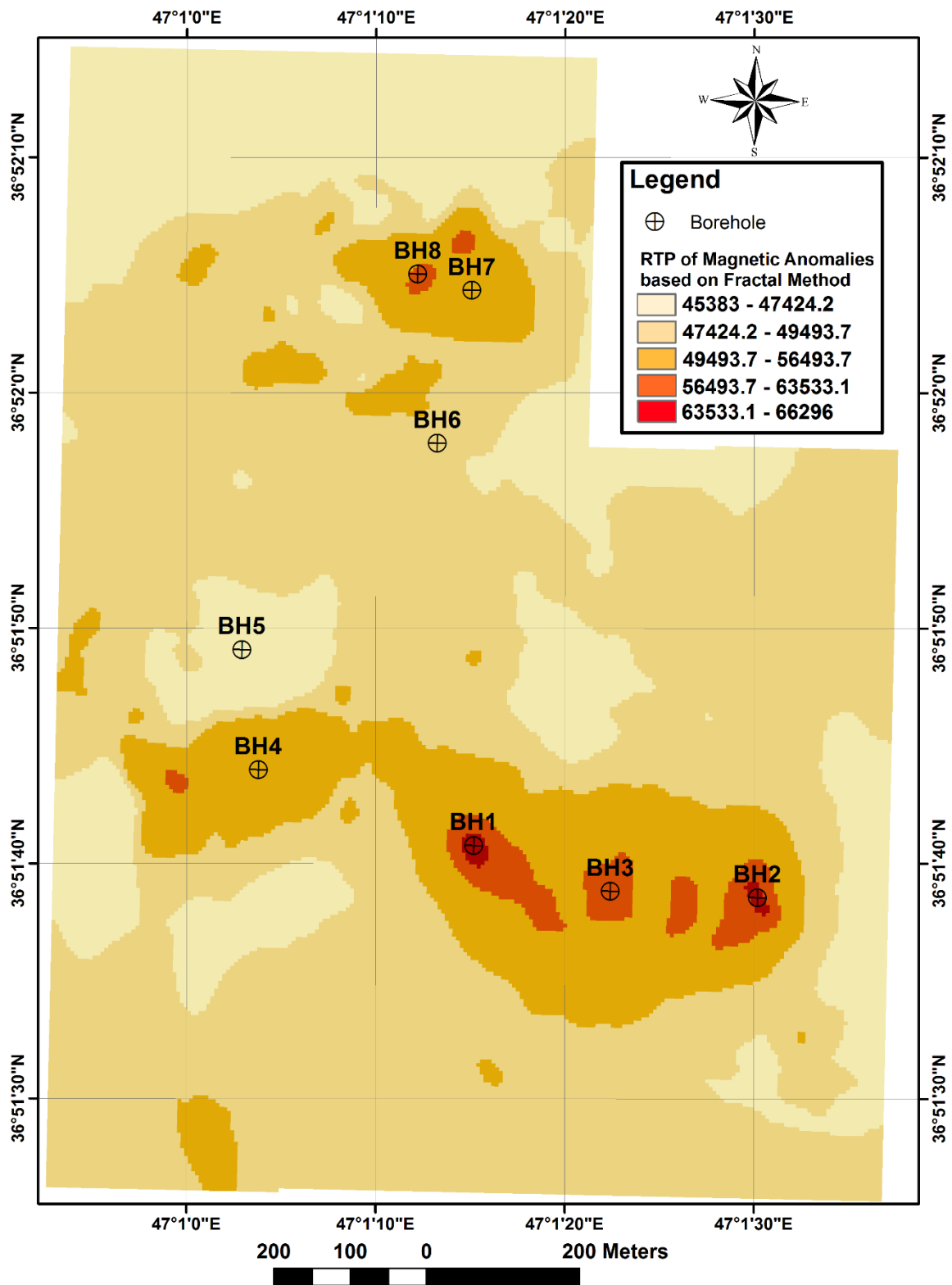
3 Figure 6. Log-log plot for RTP-MA data in Qoja-Kandi.



1

2

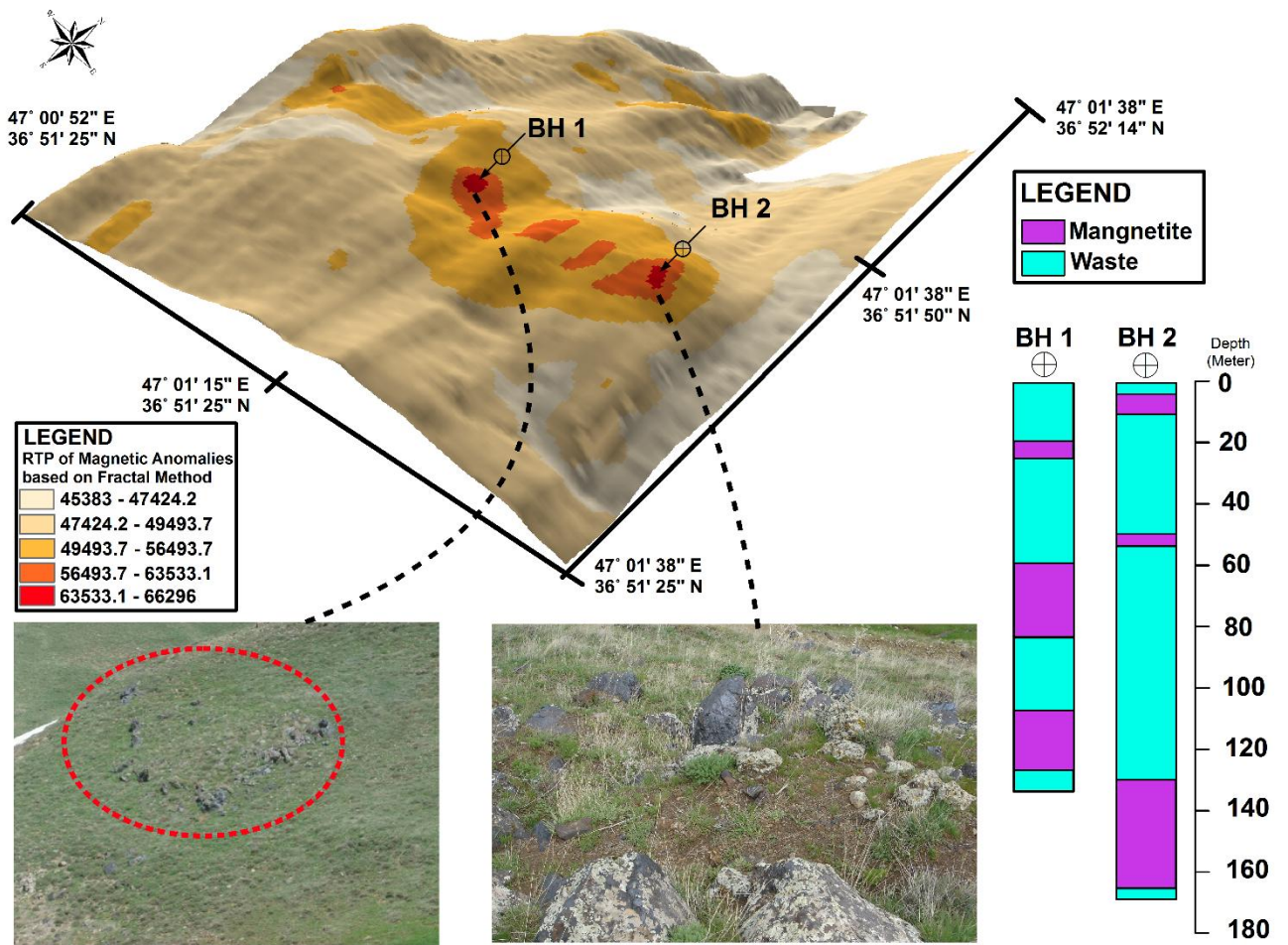
3 Figure 7. RTP map of Qoja-Kandi based on C-A method.



1

2

3 Figure 8. RTP map of Qoja-Kandi based on C-A method with drilled boreholes.



1

2

3 Figure 9. 3D RTP map of Qoja-Kandi based on C-A method with pictures from magnetite

4 zones in the surface of drilled borehole1 and 2, in addition of mentioned boreholes log plots.